Available online at www.sciencedirect.com
SCIENCE DIRECT®
Journal of Membrane Science 254 (2005) 241–248
journal of MEMBRANE SCIENCE
www.elsevier.com/locate/memsci

Improving the control of the electroless plating synthesis of Pd/Ag membranes for hydrogen separation using Rutherford backscattering

Laurens C. Witjens [a], J.H. Bitter [a], A.J. van Dillen [a], W.M. Arnoldbik [b], F.H.P.M. Habraken [b], K.P. de Jong *

[a] *Inorganic Chemistry and Catalysis, Debye Institute, Utrecht University, P.O. Box 80083, 3508 TB Utrecht, The Netherlands*
[b] *Surfaces, Interfaces and Devices, Debye Institute, Utrecht University, P.O. Box 80083, 3508 TB Utrecht, The Netherlands*

Received 13 February 2004; received in revised form 1 December 2004; accepted 3 January 2005
Available online 12 February 2005

Abstract

Rutherford backscattering (RBS) was used to determine the thickness and composition of several micrometers thick electroless-plated Pd/Ag alloy layers deposited on porous α-alumina. To determine the composition of the alloy, the thickness of the Pd layer after the first synthesis step and the thickness of the Pd/Ag sandwich structure after the second synthesis step were determined. The error in the determined thicknesses (±5%) is much smaller than for the commonly used techniques, i.e., the weight difference and the scanning electron microscopy (SEM) cross-section method. RBS allows accurate determination of plating rates and an even more accurate value for the composition, since the error in the thickness is mainly systematic. This enables one to tune the synthesis parameters for layer thickness and alloy composition.

A further and very important advantage of RBS is that pore filling of the support can be studied. Results showed that Pd penetrates into the alumina support during plating, with RBS it could be detected up to 1.4 μm deep. It is estimated that the equivalent of 0.1 μm bulk Pd is present in the pores of the support of typical electroless-plated samples.

Keywords: Rutherford backscattering; Metal layer thickness determination; Electroless plating; Pd/Ag membranes; Porosity

1. Introduction

$Pd_{77}Ag_{23}$ thin films on inert and porous supports such as α-alumina are very important membrane materials [1–4]. Applications vary from separating hydrogen from gas streams to its use in a membrane reactor in hydrogenation or dehydrogenation reactions [3,5–7]. The optimal composition for maximal hydrogen permeability has often been claimed to be 23 at.% [1,5,8–10] or in the 23–25 at.% region [11]. However, a combination of permeability data of Kikuchi and Uemiya [2,12], Knapton [11] and Darling [13] shows a plateau between about 20 and 23 at.% Ag. Furthermore, at least 20 at.% Ag is needed to prevent hydrogen embrittlement above ambient temperature [3,11,14–16]. From this we conclude that based on permeability and lifetime considerations a 20–23 at.% Ag composition is optimal. The hydrogen membrane function of pure Pd and Pd/Ag alloys is based on the solution–diffusion mechanism [3]: hydrogen molecules dissociate at its surface, the hydrogen atoms dissolve in the octahedral holes of the metal lattice and diffuse through the membrane due to the applied transmembrane hydrogen partial pressure difference to finally recombine at the opposite surface.

Because of its simplicity and relatively low costs [4,5], electroless plating is the technique of choice for large scale production of these membranes. It is a wet chemical method based on the reduction of aqueous metal ions with a suitable reducing agent such as hydrazine. The sequential electroless plating procedure commonly used to produce a Pd/Ag alloy consists of three parts: first a Pd layer is deposited, next the Pd layer is covered with an Ag layer in a second plating

* Corresponding author. Tel.: +31 30 25367662; fax: +31 30 2511027.
E-mail address: k.p.dejong@chem.uu.nl (K.P. de Jong).

0376-7388/$ – see front matter © 2005 Elsevier B.V. All rights reserved.
doi:10.1016/j.memsci.2005.01.012

and finally the metal sandwich structure is exposed to high temperatures to obtain the corresponding alloy. NH_3(aq) and $Na_2EDTA{\cdot}2H_2O$ are added to a typical electroless plating solution to set the pH and to stabilize the plating bath. With electroless plating, in contrast to electroplating, it is possible to deposit a metal film on a non-conducting support material such as alumina. Other techniques such as (bi-)sputtering [17–22] and chemical vapour deposition (CVD) [22,23] are also being used to obtain Pd/Ag mixtures for research purposes, but these techniques are less suitable for large scale production.

To optimise membrane performance both the overall thickness and the composition need to be tuned. This requires accurate measurement of the deposited amounts of Pd and Ag. In practice, there are two commonly used techniques for this purpose, viz. weight difference and scanning electron microscopy (SEM) cross-sectioning [3]. The simplest procedure is to determine the weight increase after deposition of a metal layer. However, substantial amounts of metal are deposited in the pores of the support. It cannot be established how much of this material forms an effective part of the membrane and how much can simply be bypassed by hydrogen [3]. Furthermore, it is likely that reduced metal is not the only material deposited inside the pores; significant amounts of salts may be left behind as well, leading to incorrect film thickness calculations. Alternatively, a cross-section of the sample can be studied with SEM or proton induced x-ray emission (PIXE) as Keuler et al. [8,24] have done. However, cross-sectioning, i.e., cutting or breaking the sample, will always produce deformations, which have a very strong effect on the thickness of the observed cross-section. Therefore, it can never be guaranteed that the cross-section observed with SEM is the actual thickness of the metal layer. The use of a stylus surface profiler seems to be an attractive alternative to these two techniques. It requires the creation of a so called step, the absence of metal film in a small area with edges perpendicular to the surface, either before or after the synthesis. The height difference between step bottom and top of the metal film measured with the surface profiler is considered equal to the layer thickness. However, the strong adhesion of the metal layer to the support frustrates the step creation after the synthesis and the pre-synthesis step creation would require the very problematic application of an inert step template. It is concluded that the surface profiler, the SEM cross-section and the weight difference methods cannot be used in a straightforward manner for accurate layer thickness determination for these samples.

To quantitatively determine metal layer thicknesses for this kind of samples, we apply Rutherford backscattering (RBS). In this non-destructive technique, a beam of mono-energetic ions impinges on the sample. The energy of the ions is chosen such that they can penetrate the material while having a very small probability of elastic collision with a target atom. Since conservation of energy and momentum applies, the energy of ions scattered from surface atoms is characteristic for the mass of those atoms and can easily be calculated. If collision takes place deeper in the layer, the energy of the detected ions will be smaller as a result of interactions with the atoms of the target material, thus giving RBS its depth sensitivity.

The fundamentals were discussed earlier by Pesiri et al. [25] and further information can be obtained from a number of books [26,27]. Please note that, although RBS itself is non-destructive, the samples need to be cut to fit on the sample holder and to ensure that the ion beam is perpendicular to the film surface. However, an undisturbed part of the samples has been studied in this work.

Normally, He^+ ions are used in RBS, but the probing depth is only about 1 μm in dense materials [26]. In order to achieve sufficient penetration, protons are used instead of He^+ ions. This reduces the depth resolution and mass separation. However, due to the similar masses of the isotopes of Pd and Ag the two elements cannot be distinguished from one another with RBS anyway. In order to determine the composition of Pd/Ag alloys made via the sequential electroless plating procedure, RBS measurements are performed between synthesis steps. After the first plating, the Pd layer thickness is determined and after the second plating the combined thickness of the Pd and Ag layers is obtained. The difference between the two values is the Ag layer thickness and from the ratio between this value and the total metal deposition the Ag content (at.%) of the metal deposits can be derived. Please note that the Pd deposits within the pores of the alumina support have to be taken into account for these calculations, since this amount of metal is also available for alloying during the heat treatment. Pd and Ag mix completely in all proportions [28,29] and there is no reason to assume this mixing does not occur within the pores of the support. Therefore, analogous to the work of Pesiri et al. [25] and McCleskey et al. [30] on the penetration of physical vapour deposited (PVD) Au in alumina Anodisc^{TM} membranes, the penetration depth of Pd into the α-alumina support is studied with RBS. The Pd penetration also has important ramifications for the membrane performance, i.e., on the adhesion strength of the metal layer to the support and on the hydrogen permeability. Pd penetration enhances the adhesion strength while complete pore filling results in an increase of the effective membrane thickness and consequently a decrease in hydrogen permeability.

The first step was to determine the thickness, already precisely measured with a surface profiler, of a Pd/Ag alloy layer deposited with bi-sputtering on a flat non-porous Si wafer with RBS to judge the accuracy of the ion-beam technique for this kind of samples. Secondly, a series of Pd platings with different plating times was made to reveal the effect of varying a single synthesis parameter on the RBS spectra. Finally, a complete Pd/Ag sequential plating was performed with thickness determination of the single Pd layer and the combined Pd and Ag layers, to determine the suitability of this method to tune alloy compositions. X-ray diffraction (XRD) was used to verify the composition of the alloy.

Table 1
Structure of α-alumina tube (ECN)

Layer	Thickness (μm)	Porosity (volume%)	Average pore diameter (μm)
Top	50	35	0.18
Middle	50	35	0.28
Bottom	3000	35	5

2. Experimental

2.1. Sample synthesis and characterisation

In accordance with well established procedures from literature [1,5] a number of electroless platings were performed on the outer surface of porous α-alumina tubes (length, 1 cm; o.d., 1.4 cm), activated with Pd seeds and supplied by ECN (Petten, The Netherlands). The walls of the tubes consist of three porous layers with, from the inside to the outside, decreasing pore diameters (Table 1). The surface composition of the activated α-alumina was determined with X-ray photoelectron spectroscopy (XPS) and energy dispersive X-ray analysis (EDX) was performed on a cross-section of the sample, created by fracturing the sample, to determine the bulk composition. It is important to be aware of contaminants since the interpretation of RBS results on the Pd and Ag deposits may be complicated by other heavy elements. The XPS data were obtained with a Vacuum Generators XPS system, using a CLAM-2 hemispherical analyser for electron detection. Non-monochromatic Al(Kα) X-ray radiation 2379.2×10^{-19} J (1487eV) was used for exciting the photoelectron spectra using an anode current of 20 mA at 16×10^{-16} J (10 keV). The pass energy of the analyser was set at 80×10^{-19} J (50 eV). The survey scan was taken with a pass energy of 160×10^{-19} J (100 eV). The EDX data were obtained with an FEI XL30SFEG scanning electron microscope with an EDX detector from the company EDAX. Measurements were conducted with an acceleration voltage of 15 kV and a circular spot of 5 nm diameter.

A series of Pd platings was performed, in which the plating time was the only variable. The alumina tubes were cleaned in advance in an ultrasonic bath in 96% ethanol (Lamers & Pleuger) for 15 min. The ethanol was removed with a 30 min ultrasonic bath treatment in demineralised water, which was regularly refreshed. The composition of the Pd baths is presented in Table 2. The plating times used were 30, 45, 60 and 90 min. Temperature of the baths held in a closed polypropylene vessel was kept at 323 K. Stirring was performed manually by swerving the sample holder as previous experiments had shown that Pd is occasionally deposited on the magnetic stirrer during this kind of platings. Homogeneous deposition of the metal on the alumina tubes was confirmed visually and RBS measurements (Table 4) show that very similar plating rates were achieved during the plate series. After the RBS characterisation a cross-section of the 30 min sample, created by fracturing the sample, was studied with SEM/EDX. A line scan, consisting of a 100 data points, was measured from the outer surface up to 170 μm into the sample. Again an acceleration voltage of 15 kV and a spot size of 5 nm in diameter were used.

A complete sequential plating (i.e., Pd plating followed by Ag plating) was carried out based on the results of these Pd plating time experiments, discussed in the results section. The Pd plating was conducted in accordance with the procedure and bath composition described above. Total plating time was 48 min in order to achieve a thickness of approximately 1 μm on the tube's outer surface. One part of the sample was kept for study with RBS, while the other part was plated with Ag at 323 K in a closed glass vessel using the bath composition given in Table 3. Beforehand the tube was rinsed with 96% ethanol (Lamers & Pleuger) and demineralised water. A magnetic stirrer was used during the plating to obtain more homogeneous and faster deposition of the metal. Visual inspection afterwards showed that no Ag had been deposited on the stirrer. Based on initial estimates of the amount of Pd in the pores, the plating time (57 min) was calculated from the Ag plating rate from previous measurements and aimed at a layer thickness of 500 nm to arrive at 25 at.% Ag overall composition. Finally, part of the Pd/Ag sample was set aside for study with RBS, while the other part was heated to 773 K in He atmosphere and kept at those conditions for 32 h to alloy the two metals. The progress in alloying was followed in situ with XRD measurements, after which the Ag content (at.%) was derived from the alloy peak positions and compared to the content calculated from the RBS results. Co $K\alpha_1$ XRD ($\lambda = 1.78897 \times 10^{-10}$ m (1.78897 Å)) measurements were performed using a position sensitive INEL detector (120° 2θ range) in a Bruker Nonius CPS 120 diffractometer system. Effective accuracy is estimated to be 0.1° 2θ, corresponding to an error of 3 at.% in the Ag content.

A 750 nm thick $Pd_{80}Ag_{20}$ sample on a Si wafer (with a 20 nm Ti adhesion layer) obtained with bi-sputtering [18,19], i.e., the simultaneous sputtering of two pure targets to produce a binary alloy, was received from the MESA$^+$ institute of the University Twente (Enschede, The Netherlands). The

Table 2
Pd bath composition, 1 cm tube (4.4 cm^2 surface area) per 100 ml plating solution

Component	Specification	Supplier	Quantity	Concentration (mmol l^{-1})
$PdCl_2$	59 wt.% Pd	Acros Organics	0.35 g	20
$Na_2EDTA{\cdot}2H_2O$	>99%	Aldrich	8.6 g	230
NH_3 (in H_2O)	25% (v/v)	Acros Organics	55 ml	7250
N_2H_4 (in H_2O)	51% (v/v)	Acros Organics	0.06 ml	10

Table 3
Ag bath composition, 1 cm tube (4.4 cm^2 surface area) per 200 ml plating solution

Component	Specification	Supplier	Quantity	Concentration ($mmol\,l^{-1}$)
$AgNO_3$	Pro analysis	Acros Organics	0.44 g	4
$Na_2EDTA{\cdot}2H_2O$	>99%	Aldrich	5.3 g	90
NH_3 (in H_2O)	25% (v/v)	Acros Organics	130 ml	8650
N_2H_4 (in H_2O)	51% (v/v)	Acros Organics	0.12 ml	5

alloy layer thickness was determined using a Dektak III surface profiler. The estimated error was 1–2 nm. However, the variation due to non-uniformity from the centre to the edge of the wafer (100 mm) has to be taken into account, resulting in an error of 5–10%.

2.2. Rutherford backscattering

To determine the thickness of the Pd only and Pd/Ag samples Rutherford backscattering was performed with 3.2×10^{-13} J (2 MeV) protons using a 3 MV HV Engineering accelerator. The spot used was circular with a diameter of 1 mm.

Except for the Pd/Ag bi-sputtered sample, all samples were originally tubular. A special treatment was necessary to ensure correct determination of the thicknesses. Fig. 1 illustrates the sample preparation, which consists of a series of cuts with a diamond saw and a final sanding step to obtain a level base. It is important that the angle of incidence between the ion beam and sample surface is known accurately. We opted for perpendicular incidence because this is easiest to control on these cylindrical shapes. Please note that any deviation from the angle of incidence results in a longer pathway of the ions through the metal layer and thus the thickness derived will be larger than the actual thickness. For the tube shaped samples, two to three points, carefully positioned on the perpendicular part of the surface, were measured per sample. For the bi-sputtered sample, a single RBS measurement was performed in the centre of a 5 mm × 5 mm fragment cut from the wafer. As the original location of the fragment within the wafer is unknown the upper limit of the error margin (±10%) of the surface profiler result will be used for the comparison with the RBS result.

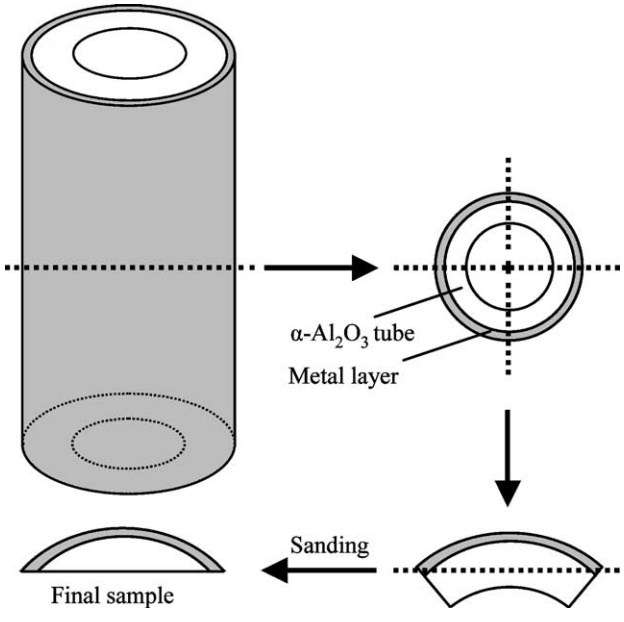

Fig. 1. Sample preparation for RBS measurements.

For reason of comparison with other techniques, it is noted that a batch of eight samples can be measured within about 4 h. This includes sample mounting on the sample holder, mounting of the sample holder into the set-up and evacuation of the set-up, which takes about 1–2 h. Actual measurement only takes a few minutes for each point. Finally, using automated data processing, the calculations only take some minutes. RBS data were processed using the RUMP source code [31]. The natural unit for RBS results is at cm^{-2}. In this work, these values are converted to layer thickness (μm) assuming the following densities: 12.02 $g\,ml^{-1}$ bulk Pd, 10.5 $g\,ml^{-1}$ bulk Ag and 3.97 $g\,ml^{-1}$ bulk alumina [32].

3. Results and discussion

3.1. XPS and SEM/EDX results

XPS measurements performed on the surface of the activated α-alumina sample showed the presence of Pd, Al and O as expected. Also some carbon and sodium, most likely deposited during synthesis, was found.

The SEM/EDX study on the cross-section of the activated α-alumina sample also showed the presence of Pd, Al, O, C and Na, and in addition Cl was detected, again most likely deposited during the synthesis. The EDX study on the cross-section of the 30 min Pd plated sample gave the same results. In Fig. 2A, a backscatter image of the sample is shown with the line of the EDX scan indicated. In Fig. 2B, the results of the line scan are shown. The Pd layer on the outer surface of the alumina can easily be observed as a white line in the backscatter image. Due to the relatively large measurement volume typical for EDX, which included a large alumina contribution, the measured maximum Pd content of the Pd layer was only 50 at.%. The Pd content decreased to 5 at.% 4.5 μm into the alumina, but the presence of Pd was detected up to much greater depths.

The SEM/EDX combination provided valuable information on our system; however, the cross-sectioning might have influenced the distribution of the Pd and comparison with the RBS results on the unperturbed sample is therefore of

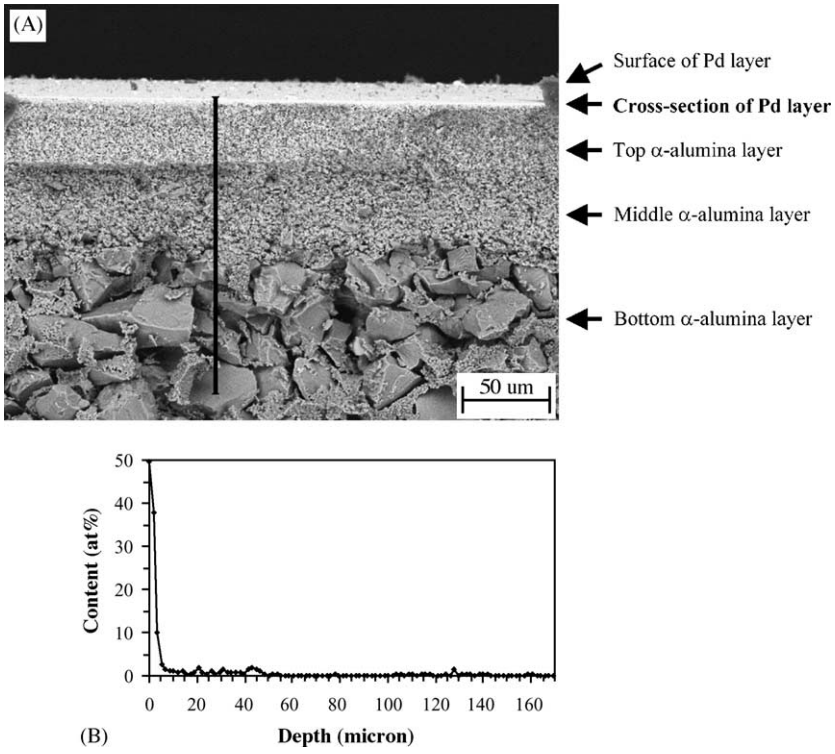

Fig. 2. (A) SEM backscatter image of cross-section of 30 min Pd plated α-alumina sample. Please note that the picture was taken under a slight angle. (B) Result of EDX Pd line scan. The line scan is indicated in (A).

great importance. Furthermore, EDX has a low accuracy, especially for the low Pd content part (<5 at.%) of the line scan. Here the error is estimated to be up to several times larger than the measured value, but also the larger line scan values should only be used qualitatively. The accuracy of EDX can only reach quantitative levels by using standards close to the sample composition with polished surfaces and measuring a polished cross-section of the sample. However, the nature of the sample makes the synthesis of appropriate standards extremely problematic and the polishing of the surface of the sample can spread Pd from the Pd layer over the alumina support. Finally, it should be noted that, in our experience, determination of the metal layer thickness with SEM is very inaccurate. As most of the film usually is deformed it is difficult to determine the position of the film edges and we estimate errors up to 50%.

3.2. RBS results

The first RBS result to be discussed is the thickness determination of the Pd/Ag bi-sputtered sample, since the thickness of this sample was already accurately known from surface profiling. In Fig. 3A, the yield of the backscattered protons is plotted against their energy. At the high energy edge the protons, which were backscattered from surface atoms of the samples, are found. These ions have not entered the sample, did not experience energy loss from travelling within the sample bulk, and therefore act as an energy reference point. In contrast, at the low energy edge protons are measured which have lost maximum energy due to bulk interactions; these protons were scattered at the metal/support interface. From the energy difference between the two edges (ΔE), determined at half height, the thickness of the metal layer can be calculated. The protons detected with an energy below 2640×10^{-16} J (1650 keV) have been backscattered from the wafer that

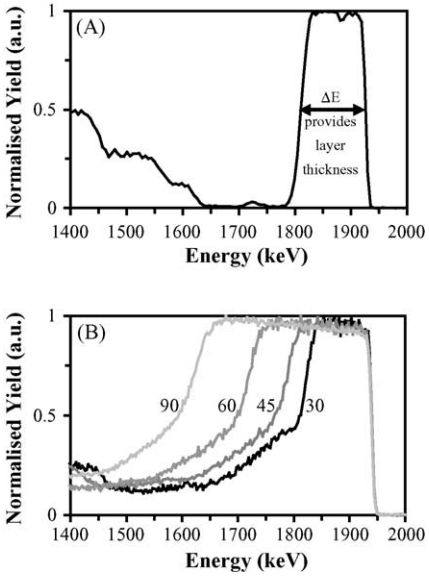

Fig. 3. RBS measurement of (A) Pd/Ag bi-sputtered sample. (B) Pd series from right to left: platetime 30 min (black), 45 min (grey), 60 min (lighter grey) and 90 min (lightest grey).

Table 4
Pd layer thicknesses derived from the RBS spectra of the Pd series

Pd plating time (min)	Layer thickness (nm)	Deposition rate (nm min^{-1})	Pd used (%)
30	730	24	1.9
45	950	21	2.5
60	1325	22	3.3
90	1900	21	4.7

supports the metal layer. The RBS measurement yielded a thickness of 720 nm, whereas the thickness measured with the surface profiler after the synthesis was 750 nm (±10%). The systematic error in the RBS results, due to uncertainties in the stopping power of the samples [26,27], is estimated at ±5%. This level of accuracy compares favourably with those of weight difference and SEM cross-sectioning.

In Fig. 3B, the averaged RBS results of the Pd plating series are shown. This figure demonstrates how an increase in metal layer thickness, going from 30 to 90 min plating time, leads to an increase in the width of the Pd backscatter peak. Note that Fig. 3A and B have different signal noise ratios. As the total measurement time is about the same for both figures this is most likely caused by a focussing difference, which resulted in a higher ion flux being directed towards the bi-sputtered sample. Table 4 shows the thicknesses calculated from the RBS spectra. From these values, we have calculated the deposition rates (nm min^{-1}) and expressed the deposited amounts of Pd as a percentage of the initial quantity of Pd in the plating bath. It is clear that the plating rate hardly varied during the experiments. Although a batch reactor was used, the amount of reactants used in the platings was only a small fraction (<5% Pd) of the available amount. The large plating solution volume/support surface ratio limited the decrease of reactant concentrations and favoured a constant plating rate.

Comparison of Fig. 3B with Fig. 3A, accentuates the shoulder at the low energy edge of the Pd plated samples (for example, for the 30 min plated sample in the 2352×10^{-16} to 2880×10^{-16} J (1470–1800 keV) area). This part of the spectra represents the Pd inside the alumina pores. The shoulders of the four samples were successfully reproduced with a RUMP simulation of Pd penetration 1400 nm into the alumina with a linear decrease of the Pd content from 30 to 5 at.%. Investigation of the Pd content deeper within the alumina is thwarted by overlap with the more intense Al signal (for the 30 min plated sample below 2352×10^{-16} J (1470 keV). The results are shown in Fig. 4.

From the 35% pore volume of the α-alumina (Table 1) and the densities of Pd (6.80×10^{22} at. ml^{-1} derived from [32]) and α-alumina (2.34×10^{22} at. ml^{-1} derived from [32]) it can be calculated that for complete filling of the pores of an alumina layer, a Pd loading of 50 at.% is required. Thus, at the 30 at.% found with the RUMP simulation the Pd can be evenly distributed over the pores, so that no pores are completely blocked, or some pores can be fully filled while others are completely empty. The two models are sketched in Fig. 5. In both models, the average membrane thickness

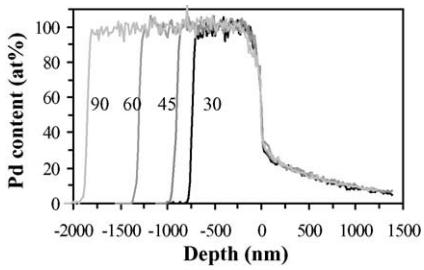

Fig. 4. RUMP simulation results for Pd series: platetime 30 min (black), 45 min (grey), 60 min (lighter grey) and 90 min (lightest grey). The depth scale is given with respect to the interface between the metal and alumina layers for easy comparison of the Pd distribution in the pores.

is increased due to the pore filling. It is therefore likely that the pore filling decreases the hydrogen permeability. However, the rapid decrease of the Pd content with the penetration depth, to 15 at.% in 500 nm, limits the extent of this influence. Significant amounts of Pd can simply be bypassed by the hydrogen. Based on Fig. 4 it is estimated that the equivalent of 100 nm of bulk Pd is present inside the alumina.

The decrease of the Pd concentration to 5 at.% over 1.4 μm as deduced from RBS is much faster than the 4.5 μm found with EDX. The RBS result is more reliable as the measurements were performed on an undisturbed part of the samples, while the EDX measurements were performed on a cross-section. Furthermore, the accuracy of RBS was demonstrated with the layer thickness determination of the Pd/Ag bi-sputtered sample, whereas the conditions required for quantitative EDX measurements could not be applied. The other two mentioned methods, weight difference and surface profiling are not very suited for pore-filling studies. The weight difference method can be used to determine the amount of material present in the pores of the alumina by simply stopping plating before substantial deposits have formed on the surface of the support. However, no information on the penetration depth can be obtained and a surface profiler will provide no information on the material present in the pores at all.

Finally, the sequential plating results are discussed. The Pd layer was found to be 1130 nm thick and, based on the pore penetration simulation results described above, it is assumed that the equivalent of 100 nm of bulk Pd was present inside

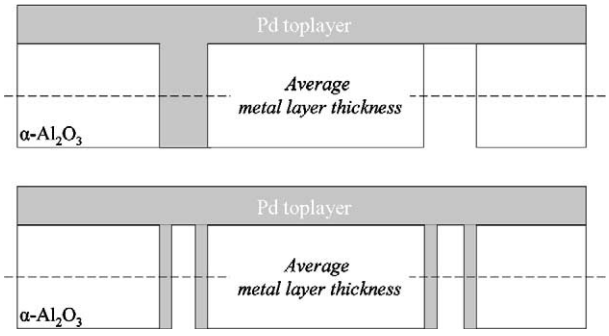

Fig. 5. Schematical representation of the two pore filling models.

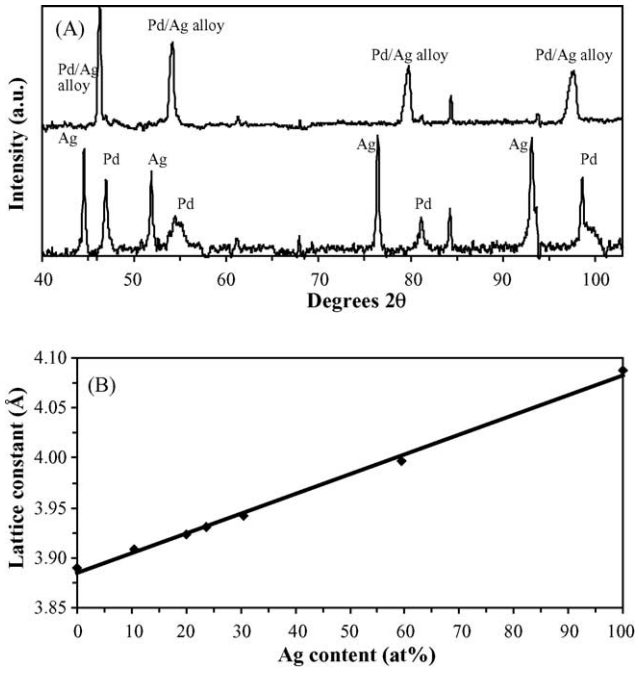

Fig. 6. (A) XRD pattern of Pd/Ag seq. plated sample; before (bottom) and after 32 h of alloying at 773 K in He (top). (B) Lattice constant vs. Ag content of Pd/Ag alloys based on [33,34].

the alumina. Although part of this material is expected not to act as part of the membrane, since it can be bypassed by the hydrogen, it most probably takes part in the alloying and must be taken into account when calculating the alloy composition. Furthermore, sintering of the Pd within the pores during the heat treatment and operational use of the membrane can cause pore blockage and an increase in the effective membrane thickness. From the total thickness of the metal deposits after Ag plating, the Ag layer thickness was determined to be 680 nm and the Ag content was subsequently calculated to be 32 at.%. Clearly, significantly more Ag has been deposited than intended. It has been our experience that the Ag plating rate can vary from batch to batch alumina tubes. A link between the surface roughness of the support, via the roughness of the Pd layer and the plating rate is suspected.

After alloying at 773 K in the in situ XRD set-up, the Ag content was determined from the alloy peak positions in the XRD pattern, shown in Fig. 6A, using the lattice constant versus Ag content diagram shown in Fig. 6B. This latter figure we derived from lattice constant data [33,34] and shows a linear relation between the lattice constant and the Ag content for Pd/Ag alloys, as predicted by Vegards law for binary alloys [35].

While the homogeneity of the Pd/Ag mixture cannot be fully assured from the XRD results, since the alloy peaks are somewhat broadened, the overall composition can be accurately determined from the position of the alloy peaks. From the pattern in Fig. 6A, the Ag content was found to be 28 ± 3 at.%. This is further proof of the accuracy of RBS and shows how the composition of alloys can be fine-tuned. In this case, by either reducing the Ag plating time or increasing the Pd plating time using deposition rate data (cf. Table 4).

4. Conclusions

Rutherford backscattering was used to determine the thickness and composition of thin Pd and Pd/Ag alloy layers deposited on porous alumina supports with electroless plating. The accuracy of 5% in the determined thicknesses is much better than for the commonly used techniques. RBS therefore allows a more accurate determination of plating rates while the determination of the Ag/Pd ratio is even more accurate since the 5% error in the thickness determination is dominantly systematic. RBS thus enables one to tune the synthesis parameters for layer thickness and alloy composition.

The RBS spectra also provided information on the penetration of Pd into the pores of the α-alumina support material, albeit with less precision than the top-layer thickness determinations. However, also in this field RBS is competitive with all existing techniques. We found that Pd penetrates the porous alumina support during plating; with RBS it could be detected up to 1.4 μm deep. The signal of deeper penetrated Pd is overlapping with the Al signal in the backscatter spectra. It is estimated that the equivalent of 100 nm of bulk Pd is present inside the alumina pores. The pores were presumably not completely filled with Pd. When used as a membrane, a significant amount of the Pd in the pores can be bypassed by hydrogen in molecular form. If the Pd plating is part of a Pd/Ag sequential plating procedure, which ends with a high temperature treatment to alloy the Pd and Ag layers, Pd inside the alumina pores probably will take part in the alloying process, as indicated by a combination of RBS and XRD measurements. Sintering of the deposits may result in extension of the effective membrane thickness.

Acknowledgements

Acknowledged are Luci Correia and Johan Overbeek (Energy research Centre of The Netherlands) for supplying the activated α-alumina tubes and for valuable discussions, Hien Duy Tong (MESA$^+$ Institute, Twente University) for supplying the Pd/Ag bi-sputtered sample and the following people of the Debye institute: R. El Ouazizi and B.S. Dauvillier for helpful discussions on the Ag plating, A.J.M. Mens for the XPS measurement, M. Versluijs-Helder for the SEM/EDX and XRD measurements and E. van der Wal for RBS support. This research was carried out under a grant from NWO-CW (Netherlands Organization for Scientific Research, Chemical Sciences) with financial contributions of Shell Global Solutions International, Senter, and the Dutch Ministry of Environmental Affairs.

References

[1] S. Uemiya, State of the art of supported metal membranes for gas separation, Sep. Purif. Methods 28 (1999) 51.

[2] S. Uemiya, T. Matsuda, E. Kikuchi, Hydrogen permeable palladium–silver alloy membrane supported on porous ceramics, J. Membr. Sci. 56 (1991) 315.

[3] S.N. Paglieri, J.D. Way, Innovations in palladium membrane research, Sep. Purif. Methods 31 (2002) 1.

[4] Y.S. Cheng, K.L. Yeung, Palladium–silver composite membranes by electroless plating technique, J. Membr. Sci. 158 (1999) 127.

[5] R. Dittmeyer, V. Höllein, K. Daub, Membrane reactors for hydrogenation and dehydrogenation processes based on supported palladium, J. Mol. Catal. A Chem. 173 (2001) 135.

[6] S. Tosti, A. Basile, G. Chiappetta, C. Rizello, V. Violante, Pd–Ag membrane reactors for water gas shift reaction, Chem. Eng. J. 93 (2003) 23.

[7] J.N. Keuler, L. Lorenzen, Comparing and modeling the dehydrogenation of ethanol in a plug-flow reactor and a Pd–Ag membrane reactor, Ind. Eng. Chem. Res. 41 (2002) 1960.

[8] J.N. Keuler, L. Lorenzen, R.D. Sanderson, V. Prozesky, W.J. Przybylowics, Characterization of electroless plated palladium–silver alloy membranes, Thin Solid Films 347 (1999) 91.

[9] H. Amandusson, L.-G. Ekedahl, H. Dannetun, Hydrogen permeation through surface modified Pd and PdAg membranes, J. Membr. Sci. 193 (2001) 35.

[10] H.-I. Chen, C.-Y. Chu, T.-C. Huang, Characterization of $PdAg/Al_2O_3$ composite membrane by electroless co-deposition, Thin Solid Films 460 (2004) 62.

[11] A.G. Knapton, Palladium alloys for hydrogen diffusion membranes, Platinum Met. Rev. 21 (1977) 44.

[12] E. Kikuchi, S. Uemiya, Preparation of supported thin palladium–silver alloy membranes and their characteristics for hydrogen separation, Gas Sep. Purif. 5 (1991) 261.

[13] A.S. Darling, Trennung und Reinigung von Wasserstoff durch permeation an membranen aus palladium-Legierungen, Chemie-Ing.-Techn. 37 (1965) 18.

[14] G.J. Grashoff, C.E. Pilkington, C.W. Corti, The purification of hydrogen, a review of the technology emphasising the current status of palladium membrane diffusion, Platinum Met. Rev. 27 (1983) 157.

[15] J.B. Hunter, Symposium on Production of Hydrogen Presented Before the ACS Division of Petroleum Chemistry, New York, American Chemical Society, 1963, p. B-49.

[16] D. Fort, J.P.G. Farr, I.R. Harris, A comparison of palladium–silver and palladium–yttrium alloys as hydrogen separation membranes, J. Less-Common Met. 39 (1975) 293.

[17] H.B. Zhao, G.-X. Xiong, G.V. Baron, Preparation and characterization of palladium-based composite membranes by electroless plating and magnetron sputtering, Catal. Today 56 (2000) 89.

[18] H.D. Tong, J.W.E. Berenschot, M.J. de Boer, J.G.E. Gardeniers, H. Wensink, H.V. Jansen, W. Nijdam, M.C. Elwenspoek, F.C. Gielens, C.J.M. van Rijn, Microfabrication of palladium–silver alloy membranes for hydrogen separation, J. Microelectromech. Syst. 12 (2003) 622.

[19] H.D. Tong, F.C. Gielens, J.G.E. Gardeniers, H.V. Jansen, C.J.M. van Rijn, M.C. Elwenspoek, W. Nijdam, Microfabricated palladium–silver alloy membranes and their application in hydrogen separation, Ind. Eng. Chem. Res. 43 (2004) 4182.

[20] B. McCool, G. Xomeritakis, Y.S. Lin, Composition control and hydrogen permeation characteristics of sputter deposited palladium–silver membranes, J. Membr. Sci. 161 (1999) 67.

[21] V. Jayaraman, Y.S. Lin, Synthesis and hydrogen permeation properties of ultrathin palladium–silver alloy membranes, J. Membr. Sci. 104 (1995) 251.

[22] G. Xomeritakis, Y.S. Lin, Fabrication of thin metallic membranes by MOCVD and sputtering, J. Membr. Sci. 133 (1997) 217.

[23] S.Y. Lu, Y.Z. Lin, Pd/Ag alloy films prepared by metallorganic chemical vapor deposition process, Thin Solid Films 376 (2000) 67.

[24] J.N. Keuler, L. Lorenzen, R.D. Sanderson, V. Prozesky, W.J. Przybylowicz, Characterising palladium–silver and palladium–nickel alloy membranes using SEM, XRD and PIXE, Nucl. Instrum. Methods Phys. Res. B 158 (1999) 678.

[25] D.R. Pesiri, R.C. Snow, N. Elliot, C. Maggiore, R.C. Dye, The characterization of assymetric alumina membranes by Rutherford backscattering spectrometry, J. Membr. Sci. 176 (2000) 209.

[26] W.K. Chu, J.W. Mayer, M.A. Nicolet, Backscattering Spectrometry, Academic Press, San Diego, 1978.

[27] J.R. Tesmer, et al., Handbook of Modern Ion Beam Analysis, Materials Research Society, Pittsburgh, 1995.

[28] I. Karakaya, W.T. Thompson, in: T.B. Massalski, H. Okamoto (Eds.), Binary Alloy Phase Diagrams, second ed., ASM International, Metals Park, 1991, pp. 55–56.

[29] F. Krüger, A. Sacklowski, X-Ray investigations of palladium–silver alloys containing hydrogen, Anal. Phys. 78 (1925) 72.

[30] T.M. McCleskey, D.S. Ehler, J.S. Young, D.R. Pesiri, G.D. Jarvinen, N.N. Sauer, Assymetric membranes with modified gold films as selective gates for metal ion separations, J. Membr. Sci. 210 (2002) 273.

[31] J.R. Doolittle, Algorithms for the rapid simulation of Rutherford backscattering spectra, Nucl. Instrum. Methods Phys. Res. Sec. B 9 (1985) 344.

[32] R.C. Weast, M.J. Astle, W.H. Beyer, Handbook of Physics and Chemistry, 64th ed., CRC Press, Boca Raton, 1983–1984.

[33] S.D. Axelrod, A.C. Makrides, X-ray studies of hydrogen–silver–palladium electrodes, J. Phys. Chem. 68 (1964) 2154.

[34] P. Eckerlin, H. Kandler, in: K.-H. Hellwege (Ed.), Landolt – Börnstein, Numerical Data and Functional Relationships in Science and Technology, Springer-Verlag, Berlin, 1971, p. 202.

[35] A.R. Denton, N.W. Ashcroft, Vegard's law, Phys. Rev. A 43 (1991) 3161.